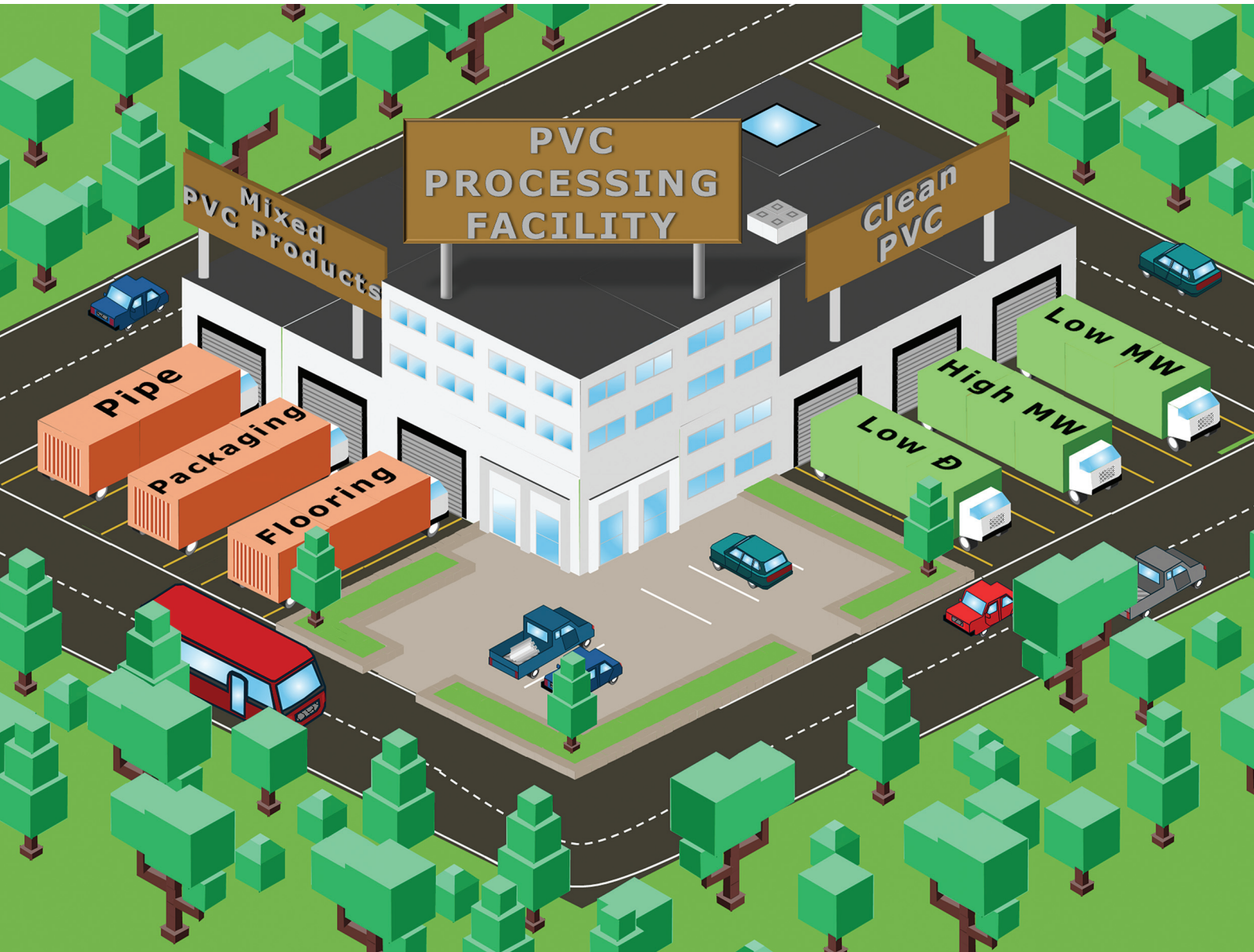


# RSC Applied Polymers

[rsc.li/RSCApplPolym](https://rsc.li/RSCApplPolym)



ISSN 2755-371X



Cite this: *RSC Appl. Polym.*, 2025, **3**, 336

## Tuning solvent strength can fractionate PVC into ultra-low molecular weight material with low dispersity†

Ali Al Alshaikh, <sup>a</sup> Jaewoo Choi, <sup>a</sup> Feranmi V. Olowookere, <sup>a</sup> Caira McClairen, <sup>b</sup> Owen G. Lubic, <sup>a</sup> Pravin S. Shinde, <sup>a</sup> C. Heath Turner <sup>a</sup> and Jason E. Bara <sup>a\*</sup>

The drive towards a circular economy in plastic materials has become a worldwide goal. It is apparent that conventional recycling alone falls well short of achieving circularity in plastic materials due to the complex formulations of commercial products. Poly(vinyl chloride) (PVC) is a post-consumer plastic that is especially challenging to recycle mechanically. However, compared to other commodity plastics, PVC is potentially well-suited for chemical recycling, especially *via* dissolution processes that selectively remove additives. Solvent-based recycling of PVC would circumvent thermomechanical processes that cause degradation of the polymer backbone. Yet, solvent-based recycling has its own set of considerations. Recycling a "Katamari" of mixed products of unknown origins (and potentially widely varying molecular weight distributions) might yield a purified PVC product that is of low value and/or without obvious utility. Thus, solvent fractionation of the feed into two or more products of relatively narrow molecular weight distributions may be required instead of bulk dissolution of the entire mass of polymer. In this work, we demonstrate solvent-based fractionation of PVC as both single-step and sequential processes. Two solvent systems were considered: acetone–methanol and tetrahydrofuran–methanol. The content of methanol in the solvent systems was varied to adjust the overall "strength" of the solvent system, thus controlling the molecular weight of the recovered soluble and insoluble fractions of PVC. Sequential fractionation proved capable of producing PVC fractions with dispersities ( $D$ ) as low as 1.14. Further, sequential fractionation of commercial PVC, containing additives, was highly promising for removing additives from the bulk (76.9%) of recovered PVC.

Received 14th October 2024,  
Accepted 20th January 2025

DOI: 10.1039/d4lp00313f

rsc.li/rscapplpolym

### 1. Introduction

The undeniable impacts of plastic pollution on the planet has charged world governments with renewed enthusiasm in dealing with end-of-life plastics. The United Nations Environment Programme<sup>1</sup> and many governments around the world<sup>2–4</sup> have already planned or taken measures toward managing plastic waste. Industry is playing its role towards a solution as well.<sup>5–9</sup> Academic interest in end-of-life plastics has also grown exponentially. Research into the "circular

economy" of plastics can be generalized by the development of new recyclable polymers<sup>10,11</sup> or products, development of sustainable (biobased) monomer production methods,<sup>12–15</sup> and the development of both open- and closed-loop recycling/upcycling methods.<sup>16,17</sup>

True closed-loop recycling is best embodied in the circularity of post-industrial and post-consumer plastic regrind for materials of known origin/composition. Solvent-based recovery is a straightforward closed-loop recycling process that could be applied to plastics where the identity of the plastic is known but the overall composition (plastic + additives) may be complex or unknown. In simple and general terms, solvent-based recovery is the use of solvents for (selective) recovery of plastics from waste.<sup>18</sup> This is done using a "strong solvent" for the dissolution of plastic from other materials which may be present (e.g., pigments, fillers). The insoluble materials are removed by filtration and clean plastic(s) is recovered *via* precipitation into an "anti-solvent". The same concept can be applied to leaching just the soluble additives (e.g. plasticizers, dyes) from waste plastics, effectively "washing" the plastic.<sup>19</sup>

<sup>a</sup>Department of Chemical & Biological Engineering, The University of Alabama, Tuscaloosa, AL 35487-0203, USA. E-mail: jbara@eng.ua.edu

<sup>b</sup>School of Chemical and Biomolecular Engineering, Georgia Institute of Technology, Atlanta, GA 30332, USA

† Electronic supplementary information (ESI) available: Summary of recent literature discussing solvent-based recycling of plastics. A discussion about computational methodologies and results. A discussion regarding the additives present in commercial PVC. Experimental spectra for GPC, FTIR, and DSC and viscosity. See DOI: <https://doi.org/10.1039/d4lp00313f>



Although not a new concept,<sup>20</sup> interest in solvent-based recovery has recently grown. This resurgence brought modern technologies<sup>21,22</sup> and techniques<sup>23</sup> to the field, with an emphasis on the use of existing<sup>24,25</sup> or new<sup>26,27</sup> “green” solvents in these processes.

Compared to mechanical recycling, solvent recovery not only promises a cleaner and more consistent<sup>28</sup> product, but also more options for controlling the form or morphology of the product obtained. Powder and pellets can be obtained using precipitation,<sup>29</sup> films can be obtained from blow spinning<sup>30</sup> or solvent casting.<sup>31,32</sup> However, solvent-based recovery has its own set of considerations that need to be addressed in order to be most effectively employed. Most methods of solvent-based recovery focus on the recovery of the entire mass of plastic (Table S1†) with removal of additives. However, unless “take-back” arrangements are made between producer and end-user(s) for specific products, simple solvent recovery methods are not likely to yield desirable results for mixed products of the same plastic. This is because dissolving two or more products made from the same plastic but with different molecular weight distributions will usually yield a material with a higher dispersity ( $D$ )<sup>33</sup> (also known as polydispersity index, PDI), which may render the recovered “pure” material much less useful. It is best to think of this method as complementary rather than competitive. Ideally, certain plastics would be sorted into their own “best” way of recovery (e.g., chemolysis of PET<sup>34</sup> or polyolefins,<sup>35</sup> and so on). To save on solvent use, solvent-based recovery can work as a complementary method to mechanical recycling,<sup>36</sup> where pure products are desired, or with tough-to-recycle wastes. While solvent-based separation of mixed plastics seems ideal, it can also be coupled with the advances in the centralized<sup>37</sup> and automated<sup>38</sup> physical sorting of plastics, which can facilitate single plastic recycling/upcycling.

Amongst the plastics that would benefit from isolation from mixed plastics is polyvinyl chloride (PVC). PVC is “anti-synergistic” (i.e., problematic) in mixed plastic recycling,<sup>39,40</sup> may contain currently prohibited substances,<sup>41</sup> and generally not collected by municipal recycling programs. Special treatment is generally needed<sup>42</sup> to prevent complications that may arise from the presence of PVC in mixed waste that is thermomechanically recycled.<sup>43,44</sup> Due to these complications and given the common presence of additives in PVC,<sup>45</sup> solvent-based recovery is particularly well-suited to PVC and has already been explored for large-scale operation. The VinyLoop process<sup>46</sup> was introduced by Solvay in 2003. Despite its closure in 2018 (due to EU phthalate regulation<sup>47</sup>), VinyLoop showed the potential of recycling by dissolution, which lead to its recent redevelopment under INEOS Inovyn.<sup>48</sup> Other new processes from CreaSolv®<sup>49</sup> and Polyloop®<sup>50</sup> indicate further current interest in solvent-based recycling of PVC. Recent work by Wagner<sup>51</sup> demonstrated successful removal of up to 99.4% of diethylhexyl phthalate (DEHP) that was originally present in PVC flooring.

Although rarely mentioned in the academic literature, a major challenge for solvent-based recovery of PVC is not pres-

ence of residual additive(s) (which in can be remedied),<sup>19</sup> but rather that commercial PVC products will come from various grades (K-values) of PVC resins that are of widely different molecular weights.<sup>52</sup> Thus, PVC recovered from recycling of mixed PVC products (using solvents, or mechanically) would likely have a much larger  $D$  than virgin resins (where typically  $D \sim 2$ ), and could make the recovered “pure” PVC less valuable and useful. Hence, a method for a fractional recovery of PVC into two or more molecular weight distributions each with  $D \leq 2$  becomes a very interesting option.

Fractionation is commonly used for lignins,<sup>53</sup> however it is less commonly applied to plastics. The still developing, yet mature, field of lignin fractionation gave rise to many fractionation methods, like fractional precipitation, pH dependent precipitation, membrane fractionation, and most commonly solvent extraction (single and sequential).<sup>53</sup> Much like lignin products,<sup>54</sup> blends of multiple PVC K-values would exhibit a broad molecular weight distribution curve. In works by Pepperl,<sup>33,55</sup> it was shown that virgin PVC contains non-negligible amounts of chains with molecular weights as low as 3 kDa (for K-50) and up to 200 kDa or more (for K-60 and K-70) (Fig. 1). Based on observations in our recent work on PVC dehydrochlorination,<sup>56</sup> we became interested in how we could selectively obtain low molecular weight chains *via* dissolution in relatively weak solvents, while also isolating the large molecular weight chains with strong solvents.

Herein, we demonstrate that solvent extraction of PVC can be used as a means of obtaining products with targeted molecular weight distributions and can yield fractions with very narrow  $D$  values (as low as  $\sim 1.1$ ). Solvent extraction was performed in both single-step and multi-step (i.e., sequential) process using a weak solvent (acetone (Ace)), a weak solvent + nonsolvent blend (Ace and methanol (MeOH)), and a strong solvent + nonsolvent blend (tetrahydrofuran (THF) and

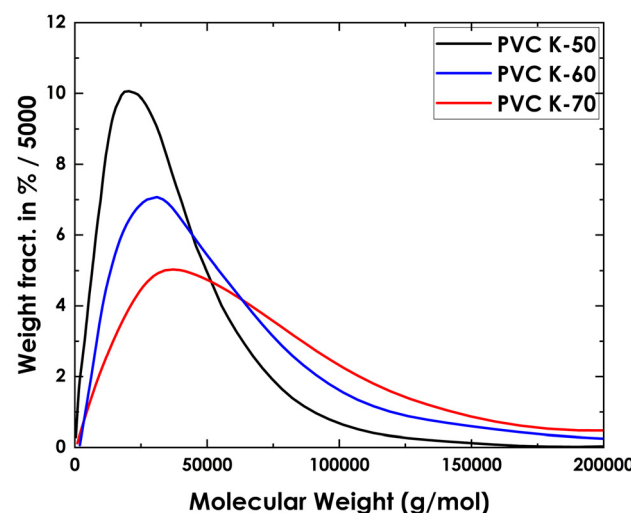


Fig. 1 Selected molecular weight distributions for virgin PVC (K-50, 60, and 70) as measured by Pepperl. Adapted with permission from Pepperl.<sup>33</sup> Copyright (2000), with permission from John Wiley and Sons.



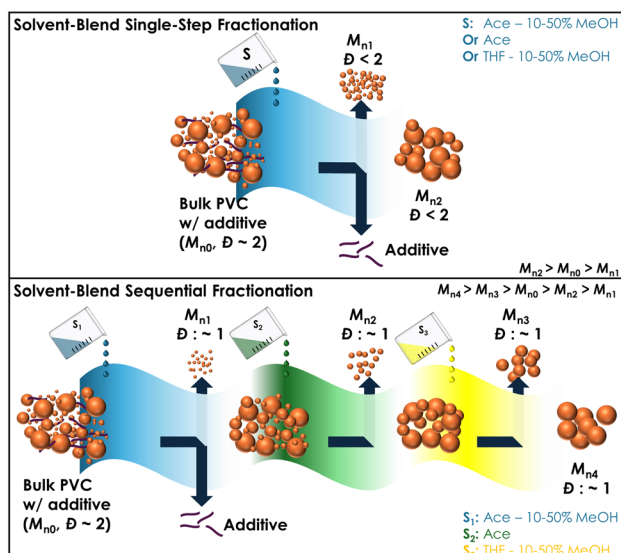


Fig. 2 Illustration of the single-step and sequential fractionation of PVC in this work.

MeOH). Single-step solvent blend extraction methods show that virgin PVC resin (K-50) can be fractionated to obtain molecular weight ranges that correspond to solvent “strength”. Sequential solvent extractions shows that PVC of low  $D$  can be fractionated from the bulk polymer, which is conceptually illustrated in Fig. 2. Further, we illustrate the viability of this method in fractionating and cleaning for commercial PVC samples (plasticized PVC and PVC pipe), which shows its potential as a recycling route for PVC. These results suggest that solvent fractionation of PVC can offer unique opportunities as the solubility of the low molecular weight fractions produced using this method can provide well-defined feedstocks for chemical modification and/or depolymerization of PVC<sup>56</sup> or back into PVC blends as melt rheology modifiers,<sup>33</sup> while the remaining (*i.e.*, insoluble) recovered clean PVC can be readily routed back as feedstock to existing applications.

Table 1 Summary of single-step fractionation experiments conducted and their designated entry IDs

Entry	PVC source	Solvent system	$M_w$ (kDa)	$M_n$ (kDa)	$D$	$T_g$ (°C)	Yield <sup>a</sup> (%)	$R_a$ <sup>b</sup> (MPa <sup>1/2</sup> )
PVC K-65 <sup>c</sup>			107	58.6	1.82	83.9	—	
F65	K-65	100% Ace	35.7	23.4	1.53	76.4	17.2	2.69
PVC K-50 <sup>c</sup>			42.8	23.3	1.83	79.1	—	
F1	K-50	50Ace : 50MeOH	4.10	3.38	1.21	58.0	2.90	16.2
F2	K-50	60Ace : 40MeOH	6.76	5.17	1.31	69.8	6.90	14.8
F3	K-50	70Ace : 30MeOH	10.1	7.57	1.34	72.8	11.8	13.5
F4	K-50	80Ace : 20MeOH	14.7	10.1	1.46	74.8	18.9	12.1
F5	K-50	90Ace : 10MeOH	20.0	13.2	1.51	76.4	29.3	9.06
F6	K-50	100% Ace	26.3	17.2	1.53	74.5	44.2	2.69
F7	K-50	50THF : 50MeOH	19.6	12.5	1.57	67.8	20.0	12.7
F8	K-50	60THF : 40MeOH	33.9	21.9	1.55	77.0	69.9	10.6
—	K-50	70THF : 30MeOH	Full dissolution with 70% THF or more					

<sup>a</sup> Yield = mass of recovered fraction/mass of starting material. <sup>b</sup>  $R_a$ : Hansen solubility parameters (HSPs) distance. <sup>c</sup> Virgin PVC resins as received from supplier.



anted, another 10 g solution of higher Ace content was added and the extraction process repeated similarly. Ace content was increased by increments of +10 wt%, until an extraction of 100% Ace was finished. The extractions were then repeated using THF-MeOH solutions starting with 50THF : 50MeOH, until all the PVC was dissolved using a solution of 70THF : 30MeOH.

#### 2.4. Sequential commercial PVC mixture fractionation

PVC pipe was first cut into small trimmings (Fig. S3†). PVC pipe trimmings and pellets were separately cleaned with water and soap, followed by washing with EtOH, and finally soaked in hexanes overnight to remove any freely soluble additives and surface coatings. PVC was then removed from hexane and allowed to dry for 2 h. Washed PVC pipe trimmings (15 g) and PVC pellets (15 g) were then moved into a glass bottle (250 mL) equipped with a stir bar. A 50Ace : 50MeOH solution (200 g) was then added to the bottle and stirred for 4 h. The solids were then allowed to settle, and the liquid phase was then carefully decanted into a funnel plugged by cotton to filter any particulates. The solution was then evaporated on a pre-weighed Pyrex dish inside a hood (~24–48 h). The extraction was then repeated similarly using solutions of increasing Ace content by increments of +10 wt%, until an extraction with 100% Ace was done. The extractions were then repeated using THF-MeOH solutions starting with 50THF : 50MeOH, until all the PVC was dissolved using a solution of 90THF : 10MeOH.

#### 2.5. Characterization

Gel permeation chromatography multi-angle laser light scattering with simultaneous refractive index (GPC-MALS-RI) was used to determine the absolute molecular weights of the PVC sources as well as the fractionation products. The measurements were performed on DAWN MALS (D8, Waters-Wyatt Technology Corporation, Goleta, CA USA) detector in HPLC grade THF at a flow rate of 1.0 mL min<sup>-1</sup> with a polarized single frequency light of 662.9 nm in conjunction with the RI detector (Model 2414, Waters-Wyatt Technology, Goleta, CA USA) using Styragel HR 5E mixed bed column (300 mm × 7.8 mm × 5 μm) for separation. The weight-average molecular weight ( $M_w$ ), the number-average molecular weight ( $M_n$ ), the dispersity ( $D = M_w/M_n$ ) and hydrodynamic radius ( $R_h$ ) of each sample was determined by the Zimm plot using the RI increment ( $dn/dc$ ) value of 0.1010 mL g<sup>-1</sup> (a standard value for PVC in THF). Astra and Empower software programs were used to run and analyze the GPC traces for MALS and RI detectors, respectively. THF was served as a mobile phase as well as solvent for dissolving PVC samples with optimized concentration of 8.0 mg mL<sup>-1</sup> and the injection volume of 80 μL. The MALS detector was operated at room temperature while the RI detector, pump oven and column oven were maintained at 40 °C. The GPC system was calibrated by using narrow distribution polystyrene standards.

Attenuated total reflection Fourier transform infrared (ATR-FTIR) was used to study the molecular structure of produced fractions, PVC sources, and additive; FTIR spectra were

obtained using the PerkinElmer Spectrum 2 instrument. Scans were acquired between 4000–400 cm<sup>-1</sup> using a resolution of 4 cm<sup>-1</sup>, and 64 accumulations.

Differential scanning calorimetry (DSC) measurements were carried out on PVC sources and fractionation products using Discovery DSC250 instrument (TA Instruments, New Castle, DE, USA) in an ultrapure (USP) N<sub>2</sub> atmosphere (20 mL min<sup>-1</sup>) at a ramp rate of 10 °C min<sup>-1</sup> with at least three heating/cooling cycles in the temperature range from -40 °C to 150 °C. Trios software (Waters Technology) was used to analyze the DSC traces to determine the thermal properties of samples such as the glass transition temperature ( $T_g$ ).

The viscosity measurements were obtained using the ViscoQC 300L PTD 100 cone-plate measurement system with a CP40 bob. Viscosity samples were prepared on a 10 : 90 polymer sample to solvent (THF) weight ratio. The instrument was calibrated with a certified reference standard (Cannon instrument) before use. The measurements were collected using a 0.5 mL polymer solution at a temperature of 20 ± 1 °C and shear rates of 10 or 100 s<sup>-1</sup> for 5 min.

#### 2.6. Computational methods

To provide molecular-level insights into the fractionation of PVC in Ace-MeOH and THF-MeOH solvent blends, molecular dynamics (MD) simulations were performed at varying MeOH % and number of PVC chains ( $n_{PVC}$ ). Table S2† outlines the system compositions used in this study. The PVC<sub>120</sub> model was employed, as it has been validated in previous studies<sup>57–59</sup> as a reliable chain length (120 repeat units) for atomistic solvated polymer simulations. While the model does not capture the full molecular weight distribution observed experimentally, it has been shown to sufficiently represent the fundamental physics of experimental systems.

The MD simulations were conducted using the Gromacs 2021.1 package.<sup>60</sup> The OPLS-AA force field<sup>61</sup> was applied to represent bonded and nonbonded interactions for PVC and the solvents. Atomic charges for PVC were derived using *ab initio* Hartree-Fock/STO-3G<sup>62</sup> in PolyParGen,<sup>63</sup> while solvent charges were obtained using B3LYP/6-31++(d,p).<sup>64</sup> van der Waals interactions were captured using the Lennard-Jones potential with a 1.0 nm cutoff, and long-range electrostatics were calculated using the particle mesh Ewald (PME) method<sup>65</sup> beyond the 1.0 nm cutoff. Geometric combination rules were applied for cross interactions.

The system configurations were built using the PACKMOL package,<sup>66</sup> followed by energy minimization *via* the steepest descent method. We then equilibrated the systems in the isothermal-isobaric (NPT) ensemble at 1 bar and 300 K for 10 ns with a time step of 1 fs, using the Parrinello-Rahman barostat<sup>67</sup> and velocity-rescaling thermostat<sup>68</sup> to maintain pressure and temperature respectively. To ensure sufficient exploration of the phase space, an annealing protocol was applied, heating the system to 600 K and cooling to 300 K over 4 cycles of 40 ns. Afterward, the systems were further equilibrated for 20 ns. Production runs were performed for 20 ns, during which configurations were extracted every 30 ps for further analyses.

Hydrogen bond lengths were constrained with the LINCS algorithm,<sup>69</sup> and periodic boundary conditions were applied in all dimensions. Detailed computational methods and calculations can be found in the ESI, Section S2.1.†

### 3. Results

### 3.1. PVC single-step fractionation by solvent-blend extraction

Unlike most solvent-based plastic recovery, fractionation offers the opportunity for selective recovery of certain “grades” of a specific plastic, based on the solvent or solvent-blend used (Fig. 3). However, among commodity plastics which bear resin identification codes (RIC) 1–6 which comprise 1 – PET (a poly-ester) and vinyl polymers (2 – HDPE, 3 – PVC, 4 – LDPE, 5 – PP, and 6 – PS), only PVC and PS have any appreciable solubility in common organic solvents at or near ambient temperature.<sup>18</sup>

Recently, we showed that K-50 and K-65 PVC were readily fractionated using either pure ethyl acetate (EtOAc) or Ace,<sup>56</sup> which we consider to be relatively weak solvents for PVC due to their inability to dissolve the entire bulk PVC (in any K-value). This led us to consider how solvent blends could be used to more finely fractionate PVC. To fractionate the lower molecular weight portions that are known to be present in K-50 and K-65 PVC,<sup>33,55</sup> extractions were done using mixtures of a weak solvent (Ace) and a non-solvent (MeOH). For higher molecular weights (short of bulk), mixtures of a strong solvent (THF) and a non-solvent (MeOH) were examined. Choice of solvents was motivated by their low boiling point for ease of

recovery, and/or their recommendation for green chemistry.<sup>70</sup> While methyl ethyl ketone (MEK or 2-butanone) is likely a better choice in the long-term as the strong solvent when considering price and green chemistry recommendations,<sup>70</sup> THF was chosen as the strong solvent for this study due to its lower boiling point and is very well-matched to PVC per Hansen solubility parameters (HSPs).<sup>71</sup>

Solvent extraction can be done as a single-step or sequential process (Fig. 2). Single-step solvent extraction is one of the most common fractionation methods owing to its simplicity. Experiments were conducted with PVC using different solvent systems (Table 1). Fractions showed a gradual increase in  $M_w$ ,  $M_n$ , and  $D$  with increase of weak solvent or strong solvent (Fig. 4 and Table 1). In all cases PVC K-50 was used, although only a 100% Ace fractionation was performed for PVC K-65.

Perhaps as expected, the weight-average molecular weight of the extracts of K-50 ( $M_w = 26.3$  kDa) and K-65 ( $M_w = 35.7$  kDa) for the 100% Ace were different, corresponding to the molecular weight distributions within the individual source material (Table 1). This seems reasonable, as source PVC with higher molecular weight would contain fewer low molecular weight chains soluble in Ace, thus shifting the average molecular weight of the associated Ace extracts. The yields of the Ace extracts reflect this as well (K-50 > K-65). Using Ace as the only solvent, 44.2% by mass was extracted from K-50 with  $D = 1.53$ , while only 17.2% by mass was extracted from K-65 with similar value of  $D = 1.53$ . Experiments on Ace extractions of K-50 and K-65 blends followed similar trends (Table S4†). The Ace extracts of the 80%

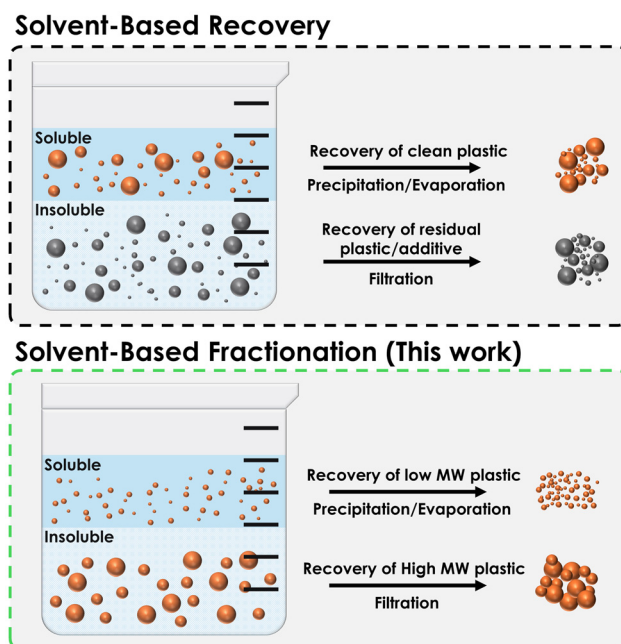


**Fig. 3** Comparison between solvent-based recovery of "whole" plastic and solvent-based fractionation of specific plastic "grades". Note that the recovery method can be reversed, with the recovered material being the insoluble (in fractionation terminology, recovery of the soluble = solvent extraction, recovery of the insoluble = fractional precipitation).

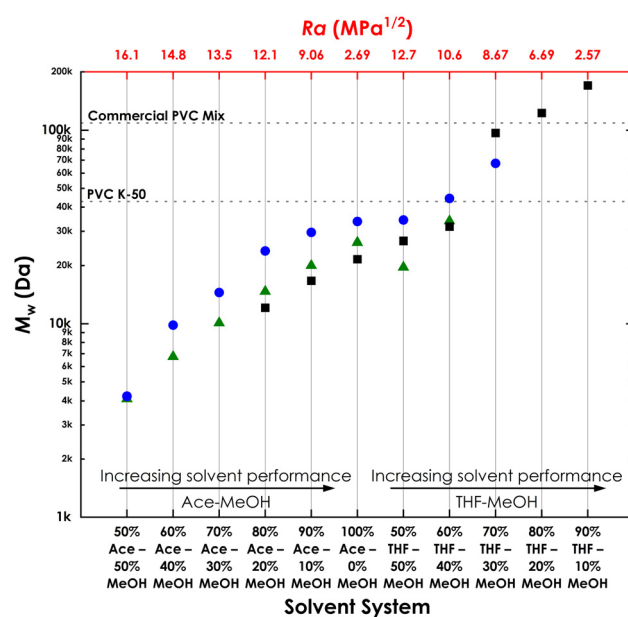


**Fig. 4** Weight average molecular weight ( $M_w$ , log scale) of (▲) PVC K-50 single-step, (●) PVC K-50 sequential and (■) commercial PVC sequential fractionations in different solvent systems. Bottom X: content of solvent systems. Top X: Hansen solubility parameters (HSPs) distance  $R_a$  (MPa $^{1/2}$ ) of corresponding solvent system (Bottom X).

K-50 : 20% K-65 blend ( $M_w = 29.9$  kDa,  $D = 1.67$ ) yielded 29.9% extracts; the 50% K-50 : 50% K-65 blend ( $M_w = 31.9$  kDa,  $D = 1.52$ ) yielded 27.2%; the 20% K-50 : 80% K-65 ( $M_w = 38.0$  kDa,  $D = 1.85$ ) yielded 15.4%. In contrast to single grade extractions, the extracts of 80% K-50 and 80% K-65 blends exhibited a relatively higher  $D$  due to the wider and asymmetrical range in molecular weight of the source material (Table S4†). Regardless, a  $D$  value  $<2$  for the blend extracts show the promise of this method for processing of mixed PVC products, regardless of source molecular weight.

### 3.2. PVC sequential fractionation by solvent-blends extraction

While single-step fractionation with Ace could be efficient for bulk recovery of the lower MW PVC chains present in a given sample, sequential fractionation could offer the ability to obtain low  $D$  fractions ( $<1.5$ ), which can be blended into specific grades when needed.<sup>33</sup> Previous sequential fractionation methods of PVC have focused on fractional precipitation.<sup>72</sup> Sequential solvent extraction fractionation was chosen here for rather logistical reasoning. In fractional precipitation, extra care needs to be placed while processing the solvent, to avoid any solvent loss, which could cause an inconsistency in further solvent blend ratios. Further, recovery of pure solvents may be complicated during fractional precipitation, especially for Ace–MeOH blends due to the presence of an azeotrope.<sup>73</sup> Hence the choice of sequential solvent extraction, as those issues are non-existent, making it a more convenient choice for processing large volumes of PVC.

In the methods presented here, PVC is contacted with the weakest solvent mixture first (here, 50Ace:50MeOH). The mixture is then separated into its liquid and solid components. The residual undissolved PVC is then contacted by an

incrementally stronger solvent mixture in increments of ~10% MeOH until it is 100% Ace. The residual PVC is then extracted in THF–MeOH blends similarly.

Similar to single-step solvent extraction, fractions see a gradual rise in the average molecular weight with increase of weak/strong solvent content (Table 2 and Fig. 4). However, the  $D$  values of the fractions were remarkably lower, and consistently  $<1.4$ , except S10 which had a  $D$  of 1.73, but contained the remaining PVC as the last fraction.

Commercial samples of PVC (pipe and plasticized pellets) were also sequentially fractionated to simulate these methods on end-of-life plastics. Both products had relatively high, but slightly different molecular weights, with PVC pipe and plasticized pellets having an  $M_w = 115$  and 105 kDa, with an  $M_n = 64.8$  and 57.1 kDa respectively, measured after removing additives (Table 2). Since the starting materials had relatively high molecular weights, no fractions were expected to be recovered for the Ace blends with 50%–30% MeOH. Nonetheless, these fractionations were attempted, and acted as selective additive extraction steps, which prevented significant contamination in subsequent fractions. The fractions produced here showed a similar trend to K-50 experiments, however, they did not have similar molecular weights. This can be attributed to the difference in molecular weight of the source materials, but also the product form. PVC pipe and pellets were extracted either as-is or after cutting to small cubes (Fig. S3†), which would interfere with the extraction process. Further, the fused/gelled behavior of commercial extruded PVC<sup>74</sup> leads to even less surface area for dissolution. PVC K-50 was received as a fine powder, which increased the surface area during the extraction. During the Ace phase of extractions, commercial PVC only gradually swelled, and only broke into powders, likely also breaking fused particles, during the THF phase of extractions. This aligns well the

**Table 2** Summary of sequential fractionation experiments conducted and their designated entry IDs

Entry	Solvent system	$M_w$ (kDa)	$M_n$ (kDa)	$D$	$T_g$ (°C)	Yield (%)	$R_a$ (MPa $^{1/2}$ )
PVC K-50 <sup>a</sup>		42.8	23.3	1.83	79.1	—	
S1	50Ace : 50MeOH	4.22	3.36	1.26	49.7	1.20	16.2
S2	60Ace : 40MeOH	9.84	8.51	1.16	67.4	5.47	14.8
S3	70Ace : 30MeOH	14.5	12.7	1.14	75.0	3.98	13.5
S4	80Ace : 20MeOH	23.8	19.4	1.22	78.1	6.32	12.1
S5	90Ace : 10MeOH	29.6	23.7	1.25	78.6	9.63	9.06
S7	100% Ace	33.7	26.0	1.29	76.6	14.1	2.69
S8	50THF : 50MeOH	34.3	24.4	1.40	77.3	3.24	12.7
S9	60THF : 40MeOH	44.4	31.5	1.41	76.9	23.1	10.6
S10 <sup>b</sup>	70THF : 30MeOH	67.4	39.1	1.73	76.5	32.4	8.67
Commercial PVC Mix <sup>a,c</sup>		109	60.5	1.80	N/A	—	
C1 <sup>d</sup>	80Ace : 20MeOH	12.1	8.28	1.46	49.6	1.0	12.1
C2	90Ace : 10MeOH	16.7	10.6	1.57	63.2	1.4	9.06
C3	100% Ace	21.6	15.4	1.40	74.0	2.1	2.69
C4	50THF : 50MeOH	26.8	21.3	1.26	70.4	0.6	12.7
C5	60THF : 40MeOH	31.7	23.3	1.36	73.3	1.9	10.6
C6	70THF : 30MeOH	96.8	62.0	1.56	80.7	46	8.67
C7	80THF : 20MeOH	123	76.4	1.61	85.0	18	6.69
C8 <sup>b</sup>	90THF : 10MeOH	170	98.0	1.73	83.0	11	2.57

<sup>a</sup> Virgin PVC or commercial products as received. <sup>b</sup> Full dissolution. <sup>c</sup> 50 : 50 mixture by weight of: PVC pellet:  $M_w = 105$  kDa,  $M_n = 57.1$  kDa,  $D = 1.84$ ,  $T_g = 81.9$  °C. PVC pipe:  $M_w = 115$  kDa,  $M_n = 64.8$  kDa,  $D = 1.78$ ,  $T_g = 84.7$  °C. <sup>d</sup> Only additives extracted using less Ace content.

relation between swelling/surface area and dissolution as explained by the Flory–Huggins theory (Section 3.6, Fig. 7).

To show the utility of the sequential fractionation process, fractions were used to formulate PVC K-50 and K-65 products by blending them with the virgin resins. For example, C3 was blended with PVC K-65 to produce a K-50 like product (Table S5†). The blend, 70% C3 and 30% K-65, had an  $M_w$  of 45.3 kDa which is 5.5% off from the K-50 resin used in this work, and 4.2% from the calculated average. In another experiment, C7 and C8 were separately blended with K-50 to produce a K-65 like product. In a 1 : 1 ratio of fraction to resin, the C7 blend had an  $M_w$  of 94.5 kDa and the C8 blend had an  $M_w$  of 99.4 kDa, which were 13% and 7.6% off from K-65 and 12% and 7.0% from the calculated average respectively.

### 3.3. Structural analysis

From spectroscopic analyses, all fractions produced during this work were identical to virgin PVC resin. For solvent-based recovery methods, the thermal or chemical degradation of the

products can be a concern. Since all extractions were run under ambient temperatures and pressures (energy inputs from sonification are likely negligible), it is highly unlikely that any thermal degradation would occur, as the degradation temperature of PVC is  $>250$  °C<sup>75</sup>. Thermal degradation of PVC typically occurs through dehydrochlorination, which releases HCl and forms conjugated sequences of C=C bonds ("polyenes") which can undergo further reactions, including cross-linking<sup>76</sup>. In all products made in this work, no sign of C=C bond formation was observed. In FTIR, C=C peaks are observed between 1600–1700  $\text{cm}^{-1}$  ( $\nu_{\text{C}=\text{C}}$ ), which are not present in any products (Fig. 5).

Chemical degradation during solvent-based recovery usually occurs as solvolysis or due to presence of additives and contaminants, introducing new structural defects. In this case, the most likely defect would be the formation of double bonds through elimination, or the formation of alcohols or ketones through oxidation. Fortunately, neither degradation routes were observed. Oxidation of PVC would cause –OH or C=O

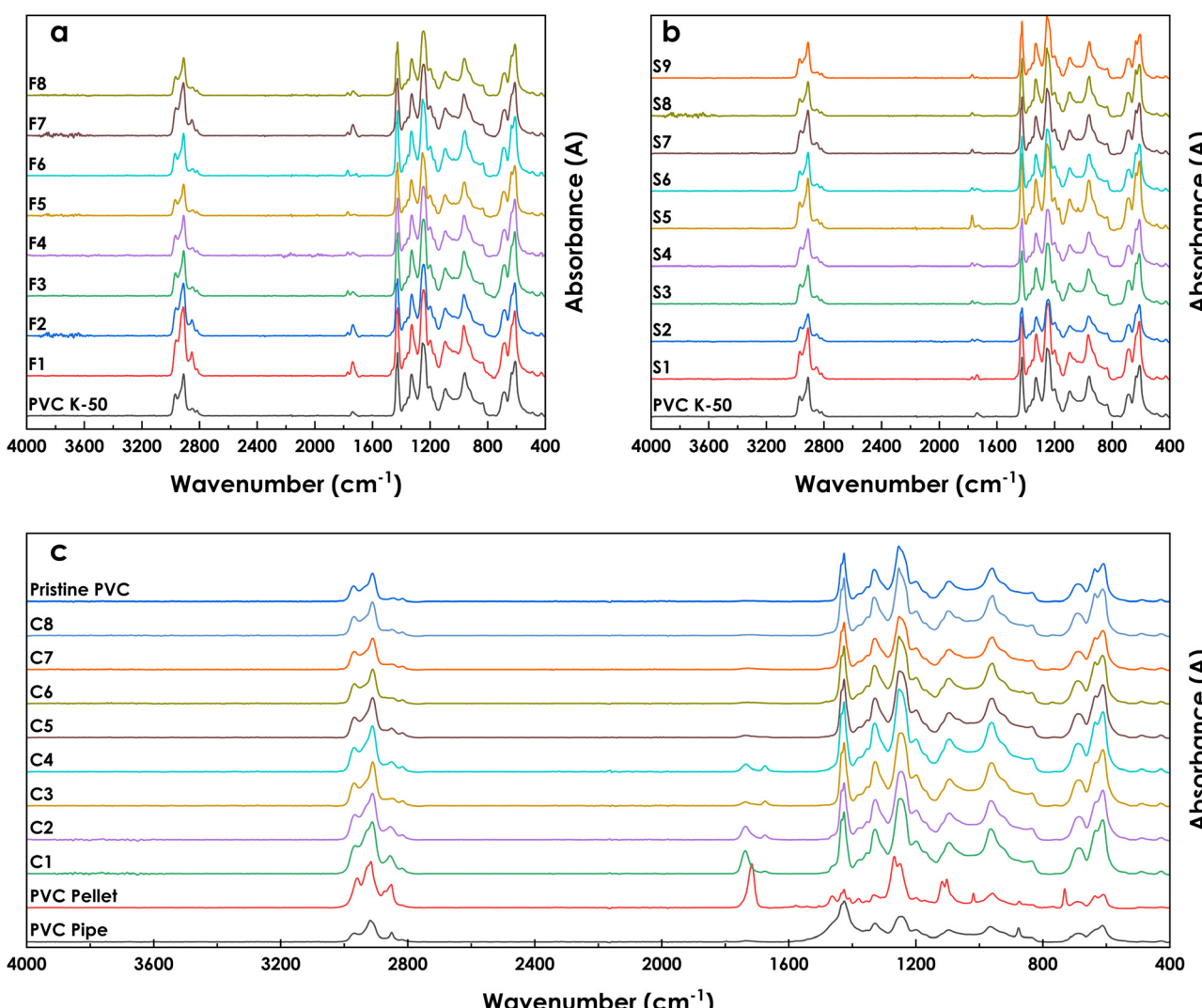


Fig. 5 FTIR spectra for (a) PVC K-50 single-step fractionation, (b) PVC K-50 sequential fractionation and (c) sequential commercial fractionation.



peaks to appear in FTIR spectra around  $3500\text{ cm}^{-1}$  ( $\nu_{\text{O}-\text{H}}$ ) and  $1700\text{--}1780\text{ cm}^{-1}$  ( $\nu_{\text{C}=\text{O}}$ ) respectively. While no  $-\text{OH}$  peaks were observed in the products, a small broad  $\text{C}=\text{O}$  peak (sometimes as two neighboring peaks) can be seen in all products and virgin resin. This  $\text{C}=\text{O}$  peak seems to be native to the PVC resin used, and is common in most PVC resins, and can be attributed to many causes as the presence of structural defects, additive, processing agents, or perhaps signals of initiator fragments at the end(s) of PVC chains.

The products made from commercial samples were analyzed for the presence of residual additives. Prior to any extractions, the source commercial PVC was soaked briefly in hexanes and MeOH to extract freely soluble plasticizers, additives, or dyes. This step removes a significant portion of the additives present in the plasticized PVC specifically (30–50%), however, that does not guarantee complete or efficient removal of all additives. So, fractionation started at a 50Aee:50MeOH solvent system, despite it not extracting any PVC, with the goal of removing as much additive as possible prior to recovering PVC. The sequential fractionation methods done with commercial samples allows for most additives to be extracted during the first fractions, with progressively less additive present in subsequent fractions. This was clear by the presence of residual additive in C1 to C4, albeit progressively less each step. This can be seen by the FTIR  $\text{C}=\text{O}$  peak around  $1740\text{ cm}^{-1}$  ( $\nu_{\text{C}=\text{O}}$ ), indicating the presence of a terephthalate ester (described as “non-*ortho* phthalate” by the vendor), and another additive peak around  $1670\text{ cm}^{-1}$  (likely  $\nu_{\text{Conjugated C}=\text{O}}$ ). The intensity and shape of the  $\text{CH}_2$  peaks around  $2780\text{--}3000\text{ cm}^{-1}$  ( $\nu_{\text{C}-\text{H}}$ ), for all fractions are PVC-like (unlike PVC pipe or PVC pellet, Fig. S8 and S9†). Which alludes to the existence of only trace amounts of additive in the contaminated fractions. Nonetheless, further purification *via* dissolution/precipitation may be required for complete removal of additives. Subsequent fractions, accounting for 76.9 wt% of the total weight of the source material, show much cleaner FTIR spectra, which were essentially identical to virgin PVC (Fig. 5c).

### 3.4. Properties

The glass transition temperatures ( $T_g$ ) of the fractionation products were measured using DSC. The dependence of  $T_g$  on the molecular weight of (linear) polymers is well understood and can be described empirically by the Flory–Fox equation.<sup>77</sup> DSC scans of PVC fractions (Section S6†) show that PVC follows this relationship as well, as can be seen in Fig. 6. The results agree well with calculated values obtained using estimates of the Flory–Fox equation parameters of PVC ( $T_{g\infty} = 351\text{ K}$  and  $K = 8 \times 10^4, 16.5 \times 10^4$ ).<sup>78</sup> Of note is the agreement of lower molecular weight fractions of commercial PVC, C2 to C4, which were shown to contain amounts of plasticizers. The exception was C1, which had a lower  $T_g$  than predicted, or observed in S1, which had a lower  $M_n$  (8.28 kDa vs. 3.36 kDa) but similar  $T_g$ , this is likely due to presence of additive in C1. This general agreement shows that the leftover plasticizer had little to no

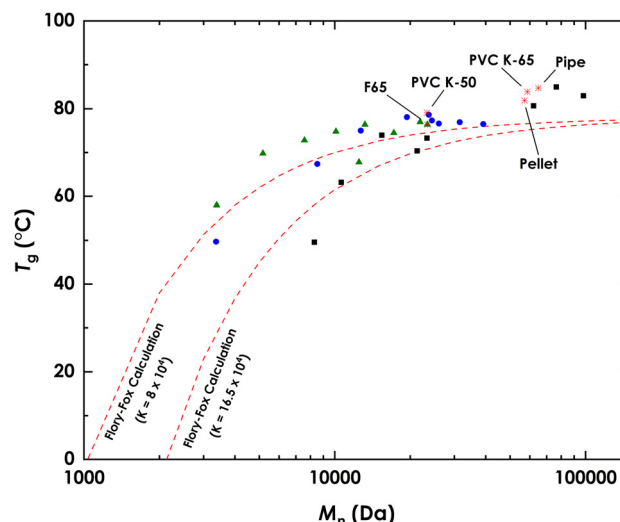


Fig. 6  $T_g$  values measured using DSC for ▲ single-step PVC K-50 fractions, ● sequential PVC K-50 fractions, ■ is sequential commercial PVC fractions, ✕ other samples (individually labeled). - - Predicted  $T_g$  values using the Flory–Fox equation.

effect on the  $T_g$  of C2 to C4, thus confirming their presence in trace amounts only.

The relationship between polymer molecular weight and polymer solution viscosity is well known.<sup>79</sup> This relationship obeys the power law, and is often described by the Mark–Houwink equation.<sup>80</sup> Solution viscosity measurements, 100 mg sample per 1 mL THF, of the acetone fractions follow this expected trend (Fig. S15†). F65 and its source PVC K-65, had a solution dynamic viscosity ( $\mu$ ) of 25.33 cP and 134.7 cP respectively; F6 and its source PVC K-50 had  $\mu$  values of 13.9 cP and 32.27 cP, respectively.

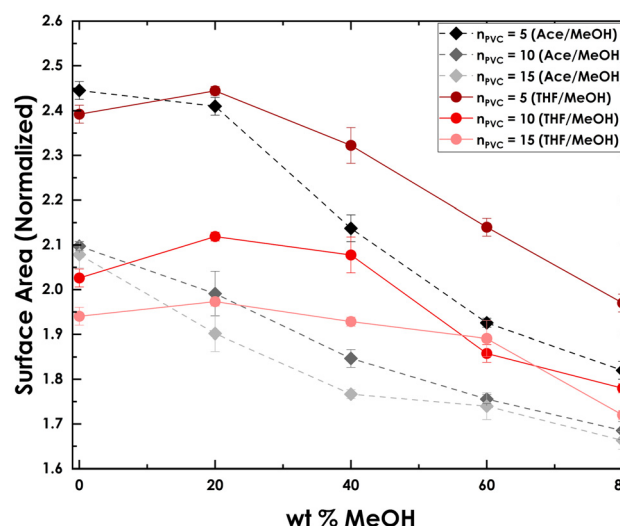


Fig. 7 Ratio of surface area for PVC in Ace–MeOH and THF–MeOH blends at different MeOH % and at different  $n_{\text{PVC}}$ .



**Table 3** Computed molar volumes ( $\text{cm}^3 \text{ mol}^{-1}$ ) and Hansen solubility parameters and various contributions (dispersion and electrostatic) in  $\text{MPa}^{1/2}$  of Ace–MeOH and THF–MeOH blends as well as bulk PVC at 300 K from MD simulations. The values in parentheses represent the experimental values of pure Ace, THF, and bulk PVC from Zeng *et al.*<sup>81</sup>

MeOH wt%	$V_m$ (Ace–MeOH)	$\delta_d^a$ (Ace–MeOH)	$\delta_e^b$ (Ace–MeOH)	$\delta_{\text{Hans}}^c$ (Ace–MeOH)	$V_m$ (THF–MeOH)	$\delta_d$ (THF–MeOH)	$\Delta_e$ (THF–MeOH)	$\delta_{\text{Hans}}$ (THF–MeOH)
0	72.40 (74.0)	17.45 (15.5)	12.91 (12.5)	21.70 (20.1)	83.52 (81.7)	17.73 (16.8)	8.28 (9.82)	19.57 (19.4)
10	68.932	16.65	14.49	22.07	75.52	17.4	10.48	20.31
20	65.12	16.46	15.94	22.91	70.16	17.01	12.36	21.03
30	62.45	15.94	17.15	23.41	68.36	16.12	14.28	21.54
40	54.92	16.14	19.06	24.97	57.91	16.44	16.95	23.61
50	51.73	15.81	20.31	25.74	53.73	16.07	18.75	24.69
60	48.95	15.47	21.48	26.47	50.36	15.65	20.35	25.67
80	44.05	14.78	23.69	27.92	44.59	14.86	23.2	27.55
$V_m$		$\delta_d$		$\delta_e$		$\delta_{\text{Hans}}$		
Bulk PVC	5351.23		18.04 (18.82)		7.56 (10.49)		19.96 (21.54)	

<sup>a</sup>  $\delta_d$ : energy from dispersion (van der Waals) interactions. <sup>b</sup>  $\delta_e^2 = \delta_p^2 + \delta_h^2$ .  $\delta_p$ : energy from polar (dipole–dipole) interactions,  $\delta_h$ : energy from hydrogen bonding interactions. <sup>c</sup>  $\delta_{\text{Hans}}$ : Hansen solubility parameter.  $\delta_{\text{Hans}}^2 = \delta_d^2 + \delta_p^2 + \delta_h^2$ .

### 3.5. Computational results

To explore the structural changes of PVC with increasing MeOH present in the solvent blends, the radius of gyration ( $R_g$ ) of PVC in Ace–MeOH and THF–MeOH was computed (Table S3†). Generally,  $R_g$  decreases with higher MeOH concentrations and with increasing  $n_{\text{PVC}}$ . Additionally, the ratio of surface area (SA) of PVC in solvent mixtures to the SA of bulk PVC was calculated (Fig. 7). A consistent decrease with increasing MeOH was observed. For instance, for  $n_{\text{PVC}} = 5$  in Ace–MeOH, the SA ratio drops from 2.45 at 0% MeOH to 1.86 at 80% MeOH. Higher  $n_{\text{PVC}}$  exhibits lower SA across all MeOH concentrations, indicating that as  $n_{\text{PVC}}$  increases, PVC chains pack more tightly, reducing solvent accessibility. The addition of MeOH likely leads to polymer chain contraction, further lowering the SA. Of note is the slope change between 20% MeOH and 40% MeOH in the THF/MeOH curves. This slope change corresponds to experimental data (Tables 1 and 2) and the stark change in solubility between 70THF : 30MeOH and 60THF : 40MeOH in C6 and C5 respectively. Data and discussion about the volume of mixing ( $V^E$ ) and the Flory–Huggins (FH) interaction parameter  $\chi_{12}$  are available as in Section S2.2.

The Hansen method (see Section S2.1†) was applied to predict PVC solubility in the mixtures. Molar volumes ( $V_m$ ) and HSP values are shown in Table 3. The  $V_m$  and HSPs of pure Ace, pure THF and bulk PVC are in very good agreement with experimental data at 300 K, validating our simulations.  $V_m$  in both mixtures decreases by a factor of ~2 as MeOH % increases, indicating that THF or Ace blends become more compact with added MeOH. Moreover, the electrostatic term increases while the dispersion term decreases, making both mixtures more polar and less compatible with PVC. Ace–MeOH shows stronger electrostatic interactions and slightly weaker dispersion interactions than THF–MeOH, making it less favorable for dissolving PVC.

Overall, the total  $\delta_{\text{hans}}$  increases with higher % MeOH, indicating reduced compatibility with PVC, as confirmed by height-

tened  $R_a$  values (Fig. S2†).  $R_a$  increases with increasing % MeOH, with THF–MeOH showing slightly smaller  $R_a$  values than Ace–MeOH.

## 4. Conclusion

PVC was successfully fractionated using weak solvent/nonsolvent and strong solvent/nonsolvent blends using commodity solvents, two of which (Ace and MeOH) are considered “green”. The fractionations were attempted using both single-step and sequential fractionation methods. Both methods showed a trend in increasing molecular weight of fraction with decrease of nonsolvent, MeOH, in solvent blends. Fractions obtained using sequential fractionation showed remarkable decrease in  $D$ , with fractions as low as  $D = 1.14$ . Further, no degradation was observed in any of the extracted samples. Commercial PVC products (e.g., pipe and pellets) were also used to illustrate the capability of this method in recovering clean PVC from formulated materials. Early “light” fractions showed slight contamination, however, the bulk of the recovered polymer, 76.9 wt%, appears identical to the pristine virgin PVC.  $T_g$  values for the recovered fractions agreed with theoretical values, constant at high  $M_n$  values but reduced greatly at low  $M_n$  values. The  $T_g$  of the low molecular weight fractions also agreed with theoretical values, proving that the presence of contaminants(plasticizers) was only in trace amounts.

The results of PVC fractionation warrant further study. Of interest, is the study and experimentation with green solvents towards fractionation.<sup>27</sup> Furthering the inspiration from the lignin fractionation field, sequential fractionation can be attempted using different solvents rather than solvent blends.<sup>82</sup> The low  $D$  of the fractions inspires study of PVC's physical properties, such as determining more accurate Flory–Fox parameters, especially at high molecular weights.



## Data availability

The data supporting this article have been included as part of the ESI.†

## Conflicts of interest

There are no conflicts to declare.

## Acknowledgements

The authors gratefully acknowledge support from the U.S. National Science Foundation (EFMA-2132133). We thank Prof. Steven T. Weinman for the use of his viscometer instrument. A. Alshaikh acknowledges the Saudi Ministry of Education as represented by the Saudi Arabian Cultural Mission (SACM) in the United States for their support. J. E. Bara acknowledges support for C. McClaren from the University of Alabama Graduate School's Strategic Graduate Partnerships Initiative (SGPI). The images within the TOC graphic were created by the authors using AI generative software (Adobe Firefly). The authors' university has a license for Adobe Firefly and terms of use associated with the software are being followed. All other images/photographs were fully created by the authors or adapted with permission.

## References

- 1 UNEP, Moving towards the end of plastic pollution, <https://www.unep.org/news-and-stories/press-release/moving-towards-end-plastic-pollution>, (accessed June, 2024).
- 2 EPA, Circular Economy | US EPA, <https://www.epa.gov/circulareconomy>, (accessed June, 2024).
- 3 C. Matthews, F. Moran and A. K. Jaiswal, *J. Cleaner Prod.*, 2021, **283**, 125263.
- 4 J. Zhu, C. Fan, H. Shi and L. Shi, *J. Ind. Ecol.*, 2019, **23**, 110–118.
- 5 PureCycle, PureCycle | The sustainable plastic revolution has arrived, <https://www.purecycle.com/>, (accessed June, 2024).
- 6 Amcor, Sustainability Packaging Solutions | Amcor, <https://www.amcor.com/sustainability>, (accessed June, 2024).
- 7 V. Institute, Advancing Circularity in the Vinyl Industry, <https://www.vinylinfo.org/circularity/>, (accessed June, 2024).
- 8 IBM, Plastic Bank | IBM, <https://www.ibm.com/case-studies/plastic-bank-systems-linuxone>, (accessed June, 2024).
- 9 Eastman, A Better Circle | Sustainable Company | Innovative Materials | Eastman, <https://www.eastman.com/en/sustainability>, (accessed June, 2024).
- 10 X. Tang and E. Y. X. Chen, *Chem.*, 2019, **5**, 284–312.
- 11 P. Shieh, W. Zhang, K. E. L. Husted, S. L. Kristufek, B. Xiong, D. J. Lundberg, J. Lem, D. Veyssset, Y. Sun, K. A. Nelson, D. L. Plata and J. A. Johnson, *Nature*, 2020, **583**, 542–547.
- 12 J.-G. Rosenboom, R. Langer and G. Traverso, *Nat. Rev. Mater.*, 2022, **7**, 117–137.
- 13 K. Bhubalan, A. M. Tamothran, S. H. Kee, S. Y. Foong, S. S. Lam, K. Ganeson, S. Vigneswari, A.-A. Amirul and S. Ramakrishna, *Environ. Res.*, 2022, **213**, 113631.
- 14 P. Benyathiar, P. Kumar, G. Carpenter, J. Brace and D. K. Mishra, *Polymers*, 2022, **14**, 2366.
- 15 R. A. Sheldon and M. Norton, *Green Chem.*, 2020, **22**, 6310–6322.
- 16 S. R. Nicholson, J. E. Rorrer, A. Singh, M. O. Konev, N. A. Rorrer, A. C. Carpenter, A. J. Jacobsen, Y. Román-Leshkov and G. T. Beckham, *Annu. Rev. Chem. Biomol. Eng.*, 2022, **13**, 301–324.
- 17 O. Horodytska, F. J. Valdés and A. Fullana, *Waste Manage.*, 2018, **77**, 413–425.
- 18 Y.-B. Zhao, X.-D. Lv and H.-G. Ni, *Chemosphere*, 2018, **209**, 707–720.
- 19 S. Ügdüler, K. M. Van Geem, M. Roosen, E. I. P. Delbeke and S. De Meester, *Waste Manage.*, 2020, **104**, 148–182.
- 20 R. J. Sperber and S. L. Rosen, *Polym. Eng. Sci.*, 1976, **16**, 246–251.
- 21 L. Wang, Y. Liu, H. Lu and Z. Huang, *Chemosphere*, 2020, **259**, 127402.
- 22 S. Yousef, M. Tatariants, M. Tichonovas, L. Kliucininkas, S.-I. Lukošiūtė and L. Yan, *J. Cleaner Prod.*, 2020, **254**, 120078.
- 23 T. W. Walker, N. Frelka, Z. Shen, A. K. Chew, J. Banick, S. Grey, M. S. Kim, J. A. Dumesic, R. C. Van Lehn and G. W. Huber, *Sci. Adv.*, 2020, **6**, eaba7599.
- 24 C. Samorì, W. Pitacco, M. Vagnoni, E. Catelli, T. Colloricchio, C. Gualandi, L. Mantovani, A. Mezzi, G. Sciuotto and P. Galletti, *Resour., Conserv. Recycl.*, 2023, **190**, 106832.
- 25 N. D. Gil-Jasso, E. A. Giles-Mazón, G. Soriano-Giles, E. W. Reinheimer, V. Varela-Guerrero and M. F. Ballesteros-Rivas, *Fuel*, 2022, **307**, 121835.
- 26 S. Qian, X. Liu, G. P. Dennis, C. H. Turner and J. E. Bara, *Fluid Phase Equilib.*, 2020, **521**, 112718.
- 27 A. Soyemi and T. Szilvási, *Ind. Eng. Chem. Res.*, 2023, **62**, 6322–6337.
- 28 J.-M. Pin, I. Soltani, K. Negrier and P. C. Lee, *Polymers*, 2023, **15**, 4714.
- 29 J. Cavalcante, R. Hardian and G. Szekely, *Sustainable Mater. Technol.*, 2022, **32**, e00448.
- 30 R. Singhal, I. Ishita and P. K. Sow, *J. Polym. Environ.*, 2019, **27**, 1240–1251.
- 31 B. A. Pulido, O. S. Habboub, S. L. Aristizabal, G. Szekely and S. P. Nunes, *ACS ACS Appl. Polym. Mater.*, 2019, **1**, 2379–2387.
- 32 M. Ramírez-Martínez, S. L. Aristizábal, G. Szekely and S. P. Nunes, *Green Chem.*, 2023, **25**, 966–977.
- 33 G. Pepperl, *J. Vinyl Addit. Technol.*, 2000, **6**, 181–186.
- 34 E. Barnard, J. J. Rubio Arias and W. Thielemans, *Green Chem.*, 2021, **23**, 3765–3789.



35 K. Faust, P. Denifl and M. Hapke, *ChemCatChem*, 2023, **15**, e202300310.

36 S. L. Nordahl, N. R. Baral, B. A. Helms and C. D. Scown, *Proc. Natl. Acad. Sci. U. S. A.*, 2023, **120**, e2306902120.

37 C. Cimpan, A. Maul, M. Jansen, T. Pretz and H. Wenzel, *J. Environ. Manage.*, 2015, **156**, 181–199.

38 S. P. Gundupalli, S. Hait and A. Thakur, *Waste Manage.*, 2017, **60**, 56–74.

39 S. Yan, D. Xia, N.-C. Lai, B. Jiang and X. Liu, *J. Hazard. Mater.*, 2023, **449**, 131032.

40 L. Chen, J. B. Moreira, L. C. Meyer and J. Szanyi, *Appl. Catal., B*, 2023, **335**, 122897.

41 K. Lewandowski and K. Skórczewska, *Polymers*, 2022, **14**, 3035.

42 P. A. Kots, B. C. Vance, C. M. Quinn, C. Wang and D. G. Vlachos, *Nat. Sustain.*, 2023, **6**, 1258–1267.

43 M. Sadat-Shojaei and G.-R. Bakhshandeh, *Polym. Degrad. Stab.*, 2011, **96**, 404–415.

44 Z. Ait-Touchente, M. Khellaf, G. Raffin, N. Lebaz and A. Elaissari, *Polym. Adv. Technol.*, 2024, **35**, e6228.

45 R. Babinsky, *Plastics, Additives and Compounding*, 2006, vol. 8, pp. 38–40.

46 VinylPlus, PVC recycling technologies, <https://www.vinyl-plus.eu/resources/pvc-recycling-technologies/>, (accessed June, 2024).

47 VINYLOOP, VINYLOOP: Closure of operation in Italy/ Phthalates issue under REACH brings down European PVC recycling project | Plasteurope.com, [https://www.plasteurope.com/news/VINYLOOP\\_t240095/](https://www.plasteurope.com/news/VINYLOOP_t240095/), (accessed June, 2024).

48 I. Inovyn, INEOS Inovyn launches next generation recycling pilot plants - to strengthen Europe's PVC recycling, <https://www.ineos.com/news/shared-news/ineos-inovyn-launches-next-generation-recycling-pilot-plants-to-strengthen-europes-pvc-recycling/>, (accessed August, 2024).

49 CreaSolv, CreaSolv: The safe solution for plastic recycling and a better environment, <https://www.creasolv.de/en/>, (accessed December, 2024).

50 Polyloop, Home - Polyloop, <https://polyloop.fr/?lang=en>, (accessed December, 2024).

51 S. Wagner and M. Schlummer, *Resour., Conserv. Recycl.*, 2024, **211**, 107889.

52 G. Wypych, in *PVC Formulary*, ed. G. Wypych, ChemTec Publishing, Toronto Ontario, 3rd edn, 2020, pp. 95–363, DOI: [10.1016/B978-1-927885-63-5.50007-0](https://doi.org/10.1016/B978-1-927885-63-5.50007-0).

53 M. Gigli and C. Crestini, *Green Chem.*, 2020, **22**, 4722–4746.

54 Q. Ma and X. Zhang, *Sci. Rep.*, 2022, **12**, 19136.

55 G. Pepperl, *Vinyl Addit. Technol.*, 2000, **6**, 88–92.

56 A. Alshaikh, S. Ezendu, D. Ryoo, P. S. Shinde, J. L. Anderson, T. Szilvási, P. A. Rupar and J. E. Bara, *ACS Appl. Polym. Mater.*, 2024, **6**, 9656–9662.

57 F. V. Olowookere, A. Al Alshaikh, J. E. Bara and C. H. Turner, *Mol. Simul.*, 2023, **49**, 1401–1412.

58 F. V. Olowookere and C. H. Turner, *Mol. Simul.*, 2024, 1–9.

59 F. V. Olowookere, G. D. Barbosa and C. H. Turner, *Ind. Eng. Chem. Res.*, 2024, **63**, 1109–1121.

60 M. J. Abraham, T. Murtola, R. Schulz, S. Pál, J. C. Smith, B. Hess and E. Lindahl, *SoftwareX*, 2015, **1**, 19–25.

61 W. L. Jorgensen, D. S. Maxwell and J. Tirado-Rives, *J. Am. Chem. Soc.*, 1996, **118**, 11225–11236.

62 J. Valatin, *Phys. Rev.*, 1961, **122**, 1012.

63 M. Yabe, K. Mori, K. Ueda and M. Takeda, *J. Comput. Chem., Jpn.*, 2019, **5**, 2018–0034.

64 J. Tirado-Rives and W. L. Jorgensen, *J. Chem. Theory Comput.*, 2008, **4**, 297–306.

65 T. Darden, D. York and L. Pedersen, *J. Chem. Phys.*, 1993, **98**, 10089–10092.

66 L. Martínez, R. Andrade, E. G. Birgin and J. M. Martínez, *J. Comput. Chem.*, 2009, **30**, 2157–2164.

67 S. Nosé and M. Klein, *Mol. Phys.*, 1983, **50**, 1055–1076.

68 G. Bussi, D. Donadio and M. Parrinello, *J. Chem. Phys.*, 2007, **126**, 014101.

69 B. Hess, H. Bekker, H. J. Berendsen and J. G. Fraaije, *J. Comput. Chem.*, 1997, **18**, 1463–1472.

70 F. P. Byrne, S. Jin, G. Paggiola, T. H. M. Petchey, J. H. Clark, T. J. Farmer, A. J. Hunt, C. Robert McElroy and J. Sherwood, *Sustainable Chem. Processes*, 2016, **4**, 7.

71 G. Grause, S. Hirahashi, H. Toyoda, T. Kameda and T. Yoshioka, *J. Mater. Cycles Waste Manage.*, 2017, **19**, 612–622.

72 H. Geerissen, J. Roos and B. A. Wolf, *Die Makromol. Chem.*, 1985, **186**, 735–751.

73 W. Xu, H. Huo, X. Ma, R. Su, Z. Yuan, X. Liang, H. Wang, T. Wen, Z. Zeng, L. Li and S. Wang, *Chem. Eng. J.*, 2023, **474**, 145565.

74 J. W. Summers, E. B. Rabinovitch and P. C. Booth, *J. Vinyl Technol.*, 1986, **8**, 2–6.

75 J. Yu, L. Sun, C. Ma, Y. Qiao and H. Yao, *Waste Manage.*, 2016, **48**, 300–314.

76 P. P. R. Cruz, L. C. da Silva, R. A. Fiúza Jr and H. Polli, *J. Appl. Polym. Sci.*, 2021, **138**, 50598.

77 T. G. Fox Jr and P. J. Flory, *J. Appl. Phys.*, 1950, **21**, 581–591.

78 X. Lu and B. Jiang, *Polymer*, 1991, **32**, 471–478.

79 A. V. Dobrynin, R. Sayko and R. H. Colby, *ACS Macro Lett.*, 2023, **12**, 773–779.

80 *Compendium of Chemical Terminology*, ed. K. Jan and C. Stuart, International Union of Pure and Applied Chemistry (IUPAC), Zürich, Switzerland, 3.0.1 edn, 2019, DOI: [10.1351/goldbook.M03706](https://doi.org/10.1351/goldbook.M03706).

81 W. Zeng, Y. Du, Y. Xue and H. Frisch, in *Physical properties of polymers handbook*, ed. J. E. Mark, Springer, New York, NY, 2007, pp. 289–303, DOI: [10.1007/978-0-387-69002-5](https://doi.org/10.1007/978-0-387-69002-5).

82 S. Y. Park, J.-Y. Kim, H. J. Youn and J. W. Choi, *Int. J. Biol. Macromol.*, 2018, **106**, 793–802.

